blood® Regular Article

HEMATOPOIESIS AND STEM CELLS

Kinase-inactivated CDK6 preserves the long-term functionality of adult hematopoietic stem cells

Isabella M. Mayer,[1] Eszter Doma,[1] Thorsten Klampfl,[1] Michaela Prchal-Murphy,[1] Sebastian Kollmann,[1] Alessia Schirripa,[1] Lisa Scheiblecker,[1] Markus Zojer,[1] Natalia Kunowska,[2] Lea Gebrail,[1] Lisa E. Shaw,[3] Ulrike Mann,[3] Alex Farr,[4] Reinhard Grausenburger,[1] Gerwin Heller,[5] Eva Zebedin-Brandl,[6] Matthias Farlik,[3] Marcos Malumbres,[7-9] Veronika Sexl,[1,10] and Karoline Kollmann[1]

[1]University of Veterinary Medicine, Vienna, Vienna, Austria; [2]Institute of Pharmaceutical Sciences, Pharmaceutical Chemistry, University of Graz, Graz, Austria; [3]Department of Dermatology, [4]Department of Obstetrics and Gynecology, [5]Clinical Division of Oncology, Department of Medicine I, and [6]Institute of Pharmacology, Centre of Physiology and Pharmacology, Medical University of Vienna, Vienna, Austria; [7]Cancer Cell Cycle Group, Vall d'Hebron Institute of Oncology, Barcelona, Spain; [8]Cell Division and Cancer Group, Spanish National Cancer Research Center, Madrid, Spain; [9]Institució Catalana de Recerca i Estudis Avançats, Barcelona, Spain; and [10]University of Innsbruck, Innsbruck, Austria

KEY POINTS

- Inhibiting CDK6 kinase function enhances long-term HSC functionality.
- Kinase-inactivated CDK6 and MAZ influence HSC maintenance.

Hematopoietic stem cells (HSCs) are characterized by the ability to self-renew and to replenish the hematopoietic system. The cell-cycle kinase cyclin-dependent kinase 6 (CDK6) regulates transcription, whereby it has both kinase-dependent and kinase-independent functions. Herein, we describe the complex role of CDK6, balancing quiescence, proliferation, self-renewal, and differentiation in activated HSCs. Mouse HSCs expressing kinase-inactivated CDK6 show enhanced long-term repopulation and homing, whereas HSCs lacking CDK6 have impaired functionality. The transcriptomes of basal and serially transplanted HSCs expressing kinase-inactivated CDK6 exhibit an expression pattern dominated by HSC quiescence and self-renewal, supporting a concept, in which myc-associated zinc finger protein (MAZ) and nuclear transcription factor Y subunit alpha (NFY-A) are critical CDK6 interactors. Pharmacologic kinase inhibition with a clinically used CDK4/6 inhibitor in murine and human HSCs validated our findings and resulted in increased repopulation capability and enhanced stemness. Our findings highlight a kinase-independent role of CDK6 in long-term HSC functionality. CDK6 kinase inhibition represents a possible strategy to improve HSC fitness.

Introduction

Hematopoietic stem cells (HSCs) are rare components of the adult bone marrow (BM), in which they preserve the hematopoietic pool by self-renewal and differentiation.[1-3] Hematopoietic stem cell transplantation (HSCT) is an essential medical procedure for various hematological diseases.[4-6] Although HSCT is a life-saving process, it has several limitations due to graft-versus-host disease or relapse.[4,5] The objective is to use the most functional and fittest HSCs for a successful HSCT.

Cyclin-dependent kinase 6 (CDK6) controls the exit from the G_1 phase of the cell cycle in all cells. The cell cycle is triggered by binding of CDK6 to D-type cyclins, which activates the kinase function of CDK6 and leads to phosphorylation of the retinoblastoma protein. Subsequent E2F-mediated transcription causes the cells to exit G_1 and enter the S phase.[7] In addition to phosphorylating retinoblastoma protein, CDK6 regulates the transcription of a range of genes in healthy and malignant cells. It does not itself bind to DNA but interacts with a plethora of transcription factors, either in a kinase-dependent or in a kinase-independent manner.[8-13] Using transgenic CDK6 animal models has been instrumental in our understanding of the complex interplay of the kinase-dependent and -independent functions of CDK6 in hematopoietic stem and progenitor cells (HSPCs).[14,15] However, we do not understand how CDK6 controls the fate of these cells.

We now report that inactivation of the kinase function of CDK6 leads to an enriched pool of quiescent HSCs with a long-term capacity to repopulate the hematopoietic system. We also show that HSCs containing a kinase-inactivated version of CDK6 retain certain features of stem cells that are lost when the HSCs lack CDK6. Our transcriptomics data provide a model to explain how CDK6 stimulates or represses various transcriptional networks to control the fate of HSCs.

Methods

Serial BM transplantation assays

A total of 5 × 10^6 *Cdk6*$^{+/+}$, *Cdk6*$^{-/-}$, or *Cdk6*$^{KM/KM}$ donor BM cells were transplanted intravenous (IV) into lethally irradiated CD45.1$^+$ recipients. The long-term repopulation capacities were evaluated after 12 weeks following transplantation by flow

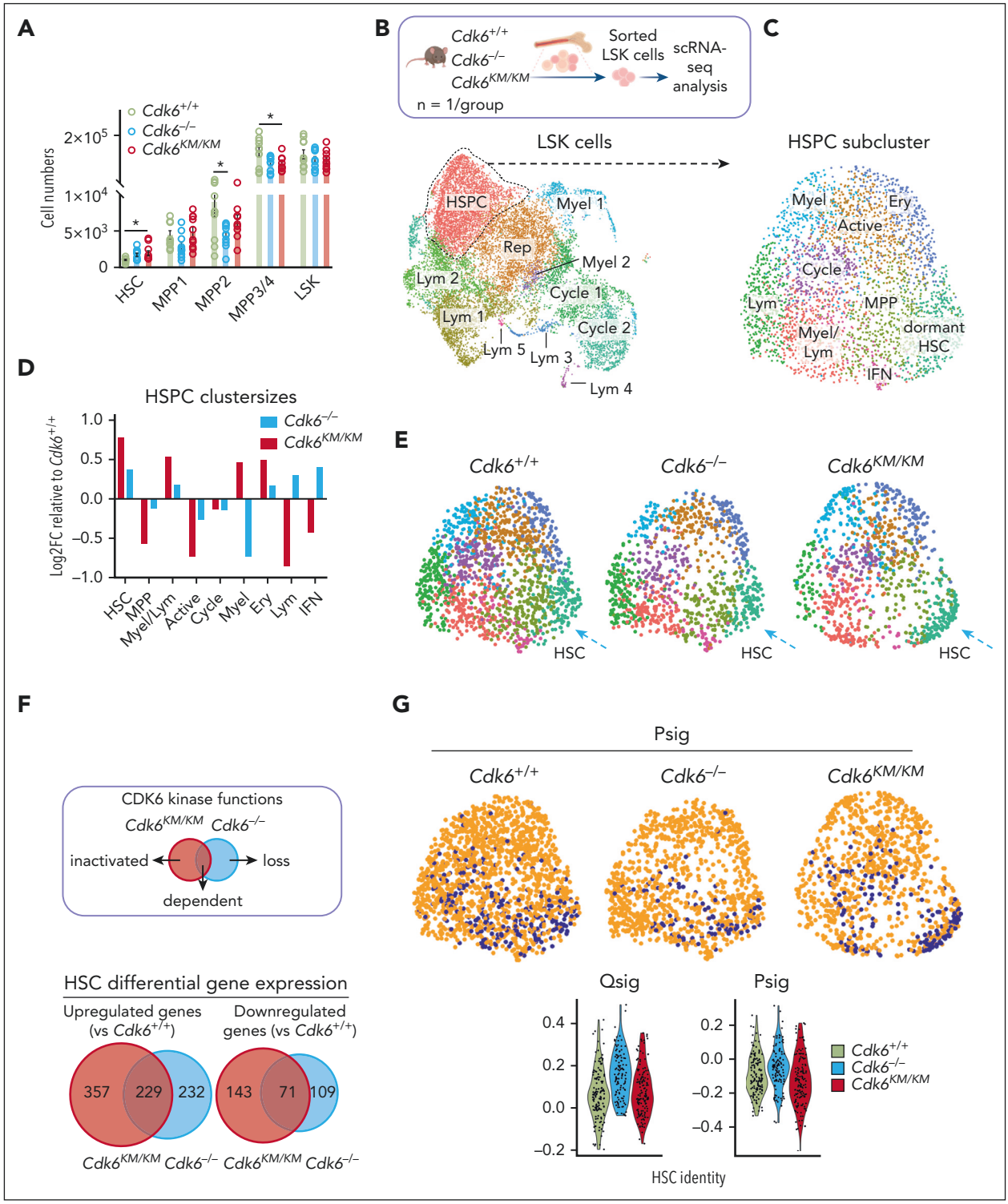

Figure 1. CDK6 shapes the HSC transcriptomic landscape in a kinase-inactivated, kinase-dependent, and -independent manner. (A) Flow cytometry analysis of isolated BM from *Cdk6*$^{+/+}$, *Cdk6*$^{-/-}$, and *Cdk6*$^{KM/KM}$ mice. Cell numbers of HSCs (LSK [Lin$^-$Sca-1$^+$c-kit$^+$] CD34$^-$CD48$^-$CD150$^+$CD135$^-$), MPP1 (LSK CD34$^+$CD48$^-$CD150$^+$CD135$^-$), MPP2 (LSK CD48$^+$CD150$^+$), and MPP 3/4 (LSK CD48$^+$CD150$^-$) (n = 10; mean ± standard error of the mean [SEM]). (B) Experimental scheme of 10x Genomics scRNA-seq including flow cytometry sorting of LSK cells of *Cdk6*$^{+/+}$, *Cdk6*$^{-/-}$, and *Cdk6*$^{KM/KM}$ BM (top). Uniform manifold approximation and projection (UMAP) visualization of 11 LSK cell clusters (bottom). Colors indicate different clusters. (C) UMAP of 9 HSPC subclusters with color code. (D) Bar chart of HSPC subcluster size differences of either *Cdk6*$^{-/-}$ or *Cdk6*$^{KM/KM}$ compared with the *Cdk6*$^{+/+}$ control (Log_2FC of percent cluster sizes relative to *Cdk6*$^{+/+}$). (E) UMAP of *Cdk6*$^{+/+}$, *Cdk6*$^{-/-}$, and *Cdk6*$^{KM/KM}$ HSPC cluster. The arrow indicates HSC subcluster. (F) Classification of CDK6 states: kinase-inactivated, kinase-dependent, and loss of CDK6 (top). Venn diagrams showing number of genes of the HSC subcluster uniquely (bottom) or commonly upregulated (left) and downregulated (right) in *Cdk6*$^{KM/KM}$ and *Cdk6*$^{-/-}$ compared with *Cdk6*$^{+/+}$ (|Log_2FC| ≥ 0.3). (G) UMAP showing *Cdk6*$^{+/+}$, *Cdk6*$^{-/-}$, and *Cdk6*$^{KM/KM}$ HSPCs overlaid with the HSC–associated proliferation gene signature (Psig).[16] The 15% of cells with the lowest Psig score (compare methods) are indicated in blue. Violin plots depict Psig and HSC–associated quiescent signature (Qsig) of all 3 genotypes. Cycle, cell cycle; Ery, erythroid; Rep, replication. *P < .05.

cytometry. For up to 4 rounds, 5 × 10^6 CD45.2$^+$ donor BM cells were re-injected in lethally irradiated CD45.1$^+$ recipient mice.

Single and repetitive pI:pC injections

Mice were injected once intraperitoneally with 10 mg/kg polyinosinic polycytidylic acid (pI:pC). Control mice were injected with the same volume of phosphate-buffered saline (PBS). Mice were dissected 18 hours after treatment, and the HSC compartment was analyzed.

For repetitive analysis, mice were serially injected intraperitoneally on every second day (3 times total) with 10 mg/kg pI:pC or PBS. Mice were dissected 2 days after the third injection.

All procedures and breeding were approved by the Ethics and Animal Welfare Committee of the University of Veterinary Medicine Vienna in accordance with the University's guidelines for Good Scientific Practice, and authorized by the Austrian Federal Ministry of Education, Science and Research (BMMWF-68.205/0093-WF/V/3b/2015, 2022-0.404.452, BMMWF-68.205/0112-WF/V/3b/2016, BMBWF-68.205/0103-WF/V/3b/2015 [TP], and 2023-0.108.862) in accordance with current legislation. The experimental protocols involving human cord blood samples were approved by the ethics committee of the Medical University of Vienna (EK1553/2014).

Other methods are described in detail in supplemental Method, available on the *Blood* website.

Results

CDK6 shapes the HSC transcriptomic landscape in a kinase-dependent and -independent manner

To understand the contribution of kinase-dependent and -independent functions of CDK6 in HSCs, we used a kinase-inactivated CDK6 K43M knockin mouse model (*Cdk6*$^{KM/KM}$),[14] which was compared with CDK6 wild type (*Cdk6*$^{+/+}$) and CDK6 knockout mice (*Cdk6*$^{-/-}$).[15] HSPC fractions of *Cdk6*$^{+/+}$ and *Cdk6*$^{KM/KM}$ mice showed comparable CDK6 protein levels (supplemental Figure 1A-C). Although BM cellularity was reduced in *Cdk6*$^{KM/KM}$ and *Cdk6*$^{-/-}$ mice, LSK (Lin$^-$Sca-1$^+$c-kit$^+$) cell numbers remained unaffected (Figure 1A; supplemental Figure 1D). HSC cell numbers were increased, and multipotent progenitor 3/4 (MPP3/4) cell numbers were reduced in the *Cdk6*$^{KM/KM}$ mice compared with *Cdk6*$^{+/+}$ mice, whereas *Cdk6*$^{-/-}$ mice showed reduced MPP2 cell numbers compared with *Cdk6*$^{+/+}$ mice (Figure 1A). *Cdk6*$^{KM/KM}$ and *Cdk6*$^{-/-}$ mice showed a significantly increased percentage of the HSC subfraction, whereas the percentage of LSK and MPP1-4 cells remained unaltered irrespective of the genotype (supplemental Figure 1E-F).

To determine underlying transcriptional changes in the HSC compartment, we performed high-resolution 10x Genomics single-cell RNA sequencing (scRNA-seq) of steady-state BM LSK cells. Data integration identified 11 individual cell clusters, which we annotated according to published marker gene expression (Figure 1B; supplemental Figure 1G).[17,18] Differences in cluster sizes were notable between *Cdk6*$^{KM/KM}$ and *Cdk6*$^{-/-}$ compared with *Cdk6*$^{+/+}$ cells (supplemental Figure 1H). In line with the known cell cycle function of CDK6,[7,14,15] the "cell cycle clusters" in *Cdk6*$^{-/-}$ and *Cdk6*$^{KM/KM}$ samples were smaller than the *Cdk6*$^{+/+}$ cluster. Flow cytometry analysis of ex vivo and cultivated *Cdk6*$^{-/-}$ and *Cdk6*$^{KM/KM}$ LSK or HSC/MPP1 cells verified reduced proliferation (supplemental Figure 1I-J).

The HSPC cluster of the scRNA-seq experiment encompassed ~20% of all LSK cells (Figure 1B). To better identify transcriptional patterns in more defined HSPCs, we reintegrated the HSPC cluster and annotated dormant HSCs and differentiation-prone cell states based on published marker genes (Figure 1C; supplemental Figure 1K).[17,18] We found 9 HSPC subclusters that exhibited transcriptional alterations, particularly in the *Cdk6*$^{KM/KM}$ mutant setting when compared with *Cdk6*$^{+/+}$ or *Cdk6*$^{-/-}$ cells. All *Cdk6*$^{KM/KM}$ clusters showed a more pronounced effect in size compared with *Cdk6*$^{-/-}$ clusters, except the cell cycle cluster. We identified opposing effects of *Cdk6*$^{KM/KM}$ and *Cdk6*$^{-/-}$ cells within the myeloid (Myel), lymphoid (Lym), and interferon (IFN) HSPC subclusters. *Cdk6*$^{KM/KM}$ and *Cdk6*$^{-/-}$ samples showed increased dormant HSCs to a similar extent as shown in Figure1A (Figure 1D). Strikingly, *Cdk6*$^{KM/KM}$ HSCs displayed a unique transcriptional pattern leading to an alternative cluster formation (Figure 1E). Differential gene expression analysis of the dormant HSC subcluster unmasked common and unique upregulated and downregulated genes in *Cdk6*$^{KM/KM}$ and *Cdk6*$^{-/-}$ compared with *Cdk6*$^{+/+}$ cells (Figure 1F). *Cdk6*$^{KM/KM}$ HSCs showed on average a reduced expression of a proliferation gene signature[16] compared with *Cdk6*$^{-/-}$ and *Cdk6*$^{+/+}$ cells (Figure 1G). *Cdk6*$^{-/-}$ cells showed a stronger expression of the quiescence-associated signature[16] compared with *Cdk6*$^{KM/KM}$ and *Cdk6*$^{+/+}$ cells. This result aligns with our previously published data, highlighting that the absence of CDK6 impairs HSC exit from their quiescent state, along with decreased response to HSC-specific stress conditions.[13] These data led us to speculate that *Cdk6*$^{KM/KM}$ HSCs respond differently to HSC-specific stress challenge compared with *Cdk6*$^{-/-}$ HSCs. Kinase-inactivated CDK6 fails to phosphorylate, despite the protein being present, which may block other kinases that compensate in a CDK6-deficient setting.

Kinase-inactivated CDK6 maintains HSPC potential upon long-term challenge

The transcriptional changes found in *Cdk6*$^{KM/KM}$ HSCs point toward alterations in IFN response and activation. We thus injected mice with a single dose of pI:pC to analyze the activation response in a short-term setting (supplemental Figure 2A). To control for the induction of Sca-1 expression by the IFN-STAT1 axis, we decided on an alternative flow cytometry gating strategy including the CD86 marker.[19] Lineage$^-$ c-kit$^+$ CD86$^+$ cell numbers were similar among the 3 genotypes upon pI:pC treatment (supplemental Figure 2B). As under steady-state conditions, HSC/MPP1-2 cell numbers were significantly higher in *Cdk6*$^{KM/KM}$ compared with *Cdk6*$^{+/+}$ mice. This was not detected for the *Cdk6*$^{-/-}$ mice (supplemental Figure 2C). *Cdk6*$^{-/-}$ HSC/MPP1 cells showed reduced G_1 cell cycle entry upon single pI:pC stimulation, in line with published data[13] (supplemental Figure 2D).

To test how *Cdk6*$^{KM/KM}$ cells respond to multiple inflammation-associated challenges, we performed serial pI:pC injections followed by serial plating assays to study long-term self-renewal (Figure 2A).

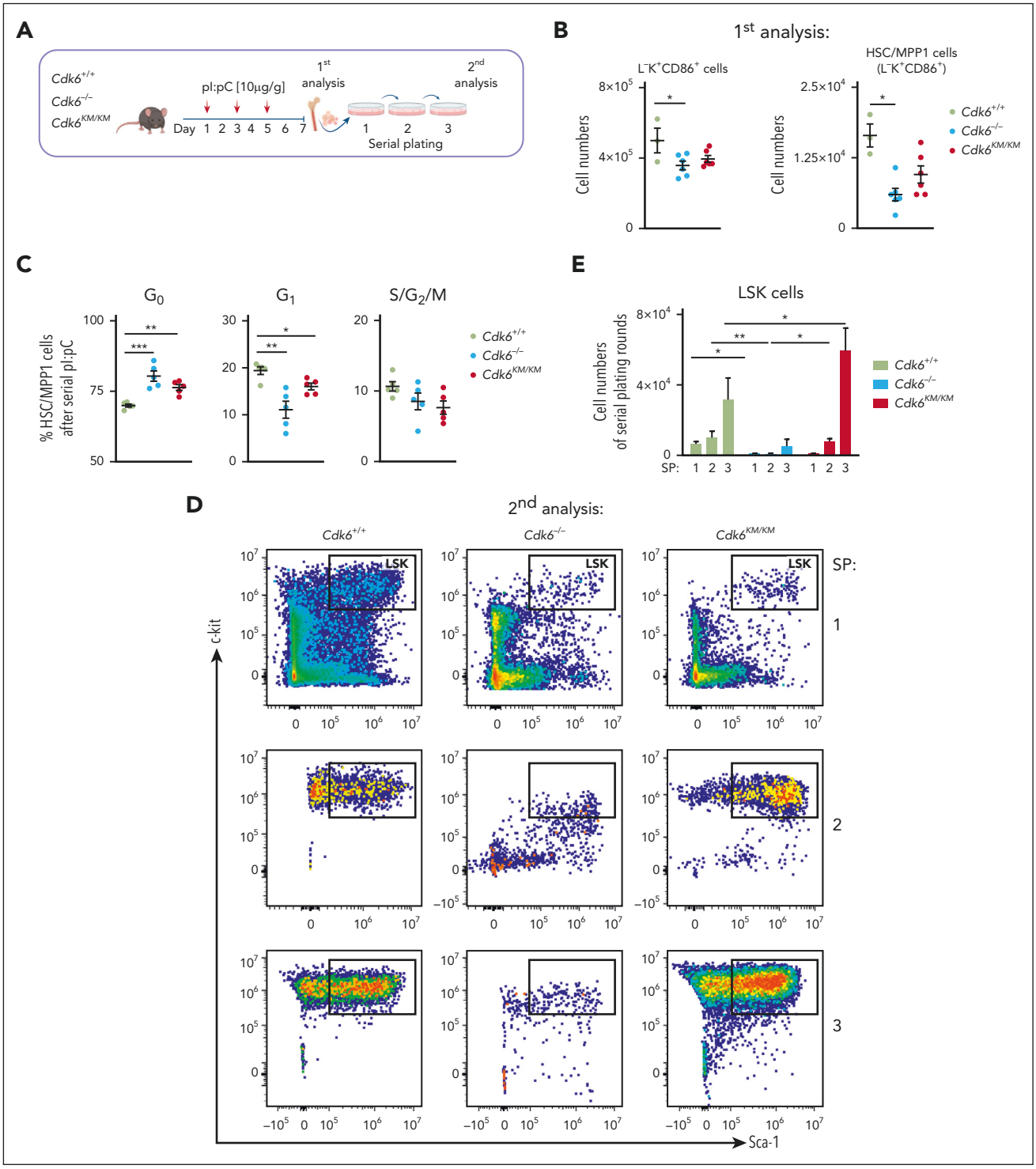

Figure 2. Kinase-inactivated CDK6 maintains HSPC potential upon long-term challenge. (A) Experimental workflow of repetitive in vivo pI:pC injections followed by an in vitro serial plating assay of *Cdk6*$^{+/+}$, *Cdk6*$^{-/-}$, and *Cdk6*$^{KM/KM}$ BM cells. (B) Flow cytometry analysis of L$^-$K$^+$CD86$^+$ and HSC-MPP1 (from L$^-$K$^+$CD86$^+$) cells upon serial pI:pC injection (n ≥ 3, mean ± SEM). (C) Cell cycle distribution of HSC/MPP1 cells upon serial pI:pC treatment (n=5, mean ± SEM). (D) Representative flow cytometry plots showing serially plated LSK cells upon repetitive pI:pC treatment. (E) Relative quantification of LSK cells during serial plating after repetitive in vivo pI:pC treatment (n = 3-6, mean ± SEM). SP, serial plating. *P < .05; **P < .01; ***P < .001.

Serial pI:pC injections resulted in decreased BM cellularity in *Cdk6*$^{-/-}$ and *Cdk6*$^{KM/KM}$ mice compared with *Cdk6*$^{+/+}$ mice, along with decreased *Cdk6*$^{-/-}$ L^{-}K^{+}CD86^{+} and HSC/MPP1 cell numbers (Figure 2B; supplemental Figure 2E). *Cdk6*$^{KM/KM}$ cells displayed intermediate numbers. MPP2-4 cells remained unchanged irrespective of the genotype (supplemental Figure 2F). A higher percentage of *Cdk6*$^{-/-}$ and *Cdk6*$^{KM/KM}$ HSC/MPP1 cells remained in the G_0 and G_1 cell cycle phases (Figure 2C). Our experimental setting was completed by serially plating BM cells into methylcellulose (Figure 2A). Serial BM cell plating revealed significantly elevated *Cdk6*$^{KM/KM}$ LSK cell numbers. In contrast, *Cdk6*$^{-/-}$ cells showed reduced LSK cell numbers and even more drastically reduced total cell numbers compared with *Cdk6*$^{+/+}$ and *Cdk6*$^{KM/KM}$ cells (Figure 2D-E; supplemental Figure 2G). *Cdk6*$^{KM/KM}$ colonies displayed an overall reduction in differentiated cells compared with *Cdk6*$^{+/+}$ and *Cdk6*$^{-/-}$ controls upon serial plating, yet *Cdk6*$^{KM/KM}$ cells were still able to produce Myel and Lym colonies (supplemental Figure 2H). The short-term and long-term pI:pC data suggest that kinase-inactivated CDK6 mimics full loss of CDK6 in regard to cell cycle, which can be observed most prominently in a short-term activation setting. However, in a repetitive activation setting, where long-term stem cell properties come into account, kinase-inactivated CDK6 maintained LSK numbers, whereas loss of CDK6 led to reduced LSK cell numbers. The advantage of *Cdk6*$^{KM/KM}$ HSCs comes with only mild expenses regarding the differentiation potential.

Kinase-inactivated CDK6 enhances HSC homing and self-renewal

Angiopoietin 1 (Angpt1) was 1 of the most upregulated genes in *Cdk6*$^{KM/KM}$ compared with *Cdk6*$^{+/+}$ and *Cdk6*$^{-/-}$ cells from the dormant HSC subcluster (Figure 3A). As Angpt1/Tie2 is a critical signaling component for HSC quiescence and homing,[20,21] we tested whether kinase-independent functions of CDK6 affect homing and migration of HSCs (supplemental Figure 3A). Sorted LSK cells were plated in a transwell system including stromal cell-derived factor 1α as an attractant. No changes in migration of the total LSK compartment were observed. When analyzing HSC/MPP1 cells, *Cdk6*$^{KM/KM}$ cells migrated significantly more than *Cdk6*$^{-/-}$ HSC/MPP1 cells in vitro. Therefore, we performed an in vivo homing assay. We injected CD45.2^{+} LSK cells of *Cdk6*$^{+/+}$, *Cdk6*$^{-/-}$, and *Cdk6*$^{KM/KM}$ mice IV into CD45.1^{+} recipient mice (Figure 3B). Injected CD45.2^{+} LSK and MPP2-4 progenitor cells were similarly present in the BM irrespective of the genotype 18 hours thereafter (Figure 3C; supplemental Figure 3B). In contrast, significantly more *Cdk6*$^{KM/KM}$ HSC/MPP1 cells homed to the BM compared with *Cdk6*$^{+/+}$ and *Cdk6*$^{-/-}$ HSC/MPP1 cells.

Self-renewal and homing are processes involved in HSC engraftment. To assess the repopulation capacity of *Cdk6*$^{KM/KM}$ HSC/MPP1 cells, we serially transplanted BM cells from CD45.2^{+} *Cdk6*$^{+/+}$, *Cdk6*$^{-/-}$, and *Cdk6*$^{KM/KM}$ mice into lethally irradiated CD45.1^{+} recipient mice (Figure 3D). From the second round of transplantation onward, we identified significantly higher numbers of donor-derived *Cdk6*$^{KM/KM}$ LSK cells compared with *Cdk6*$^{+/+}$ and *Cdk6*$^{-/-}$ LSK cells (Figure 3E-F). This effect was even more pronounced for the HSC/MPP1 cell compartment (Figure 3G). In contrast to *Cdk6*$^{KM/KM}$ cells, *Cdk6*$^{-/-}$ LSK and HSC/MPP1 cells significantly declined over serial rounds of transplantation. *Cdk6*$^{KM/KM}$ MPP2-4 progenitor cells displayed higher percentages of BM engraftment compared with *Cdk6*$^{-/-}$ MPP2-4 cells within all transplantation rounds (supplemental Figure 3C). No significant differences in the MPP2-4 cells were observed between *Cdk6*$^{KM/KM}$ and CDK6 wild-type cells.

Comparable percentages of Myel and Lym cells were found upon repopulation of *Cdk6*$^{+/+}$ and *Cdk6*$^{KM/KM}$ cells in the long-term transplantation setting (Figure 3H). Of note, *Cdk6*$^{-/-}$ cells showed a shift from the Myel to the Lym lineage, with the strongest effect observed in the second serial transplantation round. These data are consistent with the enhanced Lym HSPC subcluster identified by the scRNA-seq data (Figure 1D). No significant alterations were detected in the composition of the peripheral blood (supplemental Figure 3D). To further investigate the functionality of CDK6 kinase-inactivated HSC/MPP1 cells, we performed competitive transplantation assays with *Cdk6*$^{KM/KM}$ or *Cdk6*$^{+/+}$ BM cells (Figure 3I). *Cdk6*$^{KM/KM}$ HSC/MPP1 cells showed a competitive advantage compared with control counterparts (Figure 3J). No major differences in the MPP2-4 fractions and LSK cells between *Cdk6*$^{+/+}$ and *Cdk6*$^{KM/KM}$ were observed (supplemental Figure 3F-G). These results highlight a specific role for kinase-inactivated CDK6 in the repopulation ability of HSCs, which is not mimicked by full loss of CDK6. *Cdk6*$^{KM/KM}$ HSCs balance proliferation, differentiation, and self-renewal through a unique mechanism of transcriptional regulation.

Kinase-inactivated CDK6 balances quiescent and activated transcriptional programs of long-term HSCs

To gain deeper insights into how kinase-inactivated CDK6 protects HSCs during long-term challenge, we performed low-input RNA-seq of flow cytometry–sorted serially transplanted (second round) HSC/MPP1 cells (Figure 4A). *Cdk6*$^{KM/KM}$ and *Cdk6*$^{-/-}$ cells showed unique and common transcriptional changes (Figure 4B). From the scRNA-seq analysis, we identified a gene set associated with kinase-inactivated CDK6, kinase-dependent activity, and CDK6 loss. We first defined gene sets associated with HSC quiescence or HSC activation (supplemental Figure 4A).[22] *Cdk6*$^{KM/KM}$ and *Cdk6*$^{+/+}$ HSC/MPP1 cells displayed a positive enrichment of the quiescent stem cell gene set compared with *Cdk6*$^{-/-}$ HSC/MPP1 cells (Figure 4C). This finding reflected the reduced engraftment potential of the *Cdk6*$^{-/-}$ HSC/MPP1 cells over *Cdk6*$^{KM/KM}$ and *Cdk6*$^{+/+}$ HSC/MPP1 cells (Figure 3G). A significant negative enrichment of the activation stem cell gene set was identified for *Cdk6*$^{KM/KM}$ and *Cdk6*$^{-/-}$ HSC/MPP1 cells compared with *Cdk6*$^{+/+}$ HSC/MPP1 cells, which aligns with the proliferation-associated gene signature from the dormant HSC cluster (Figure 1G and 4D). These results highlight the importance of kinase-independent effects of CDK6 in maintaining quiescent gene expression patterns, which becomes critical under HSC long-term behavior. Under homeostasis, we previously observed the regulation of the *Cdk6*$^{KM/KM}$ and *Cdk6*$^{-/-}$ quiescent genes. In these conditions, we identified a different

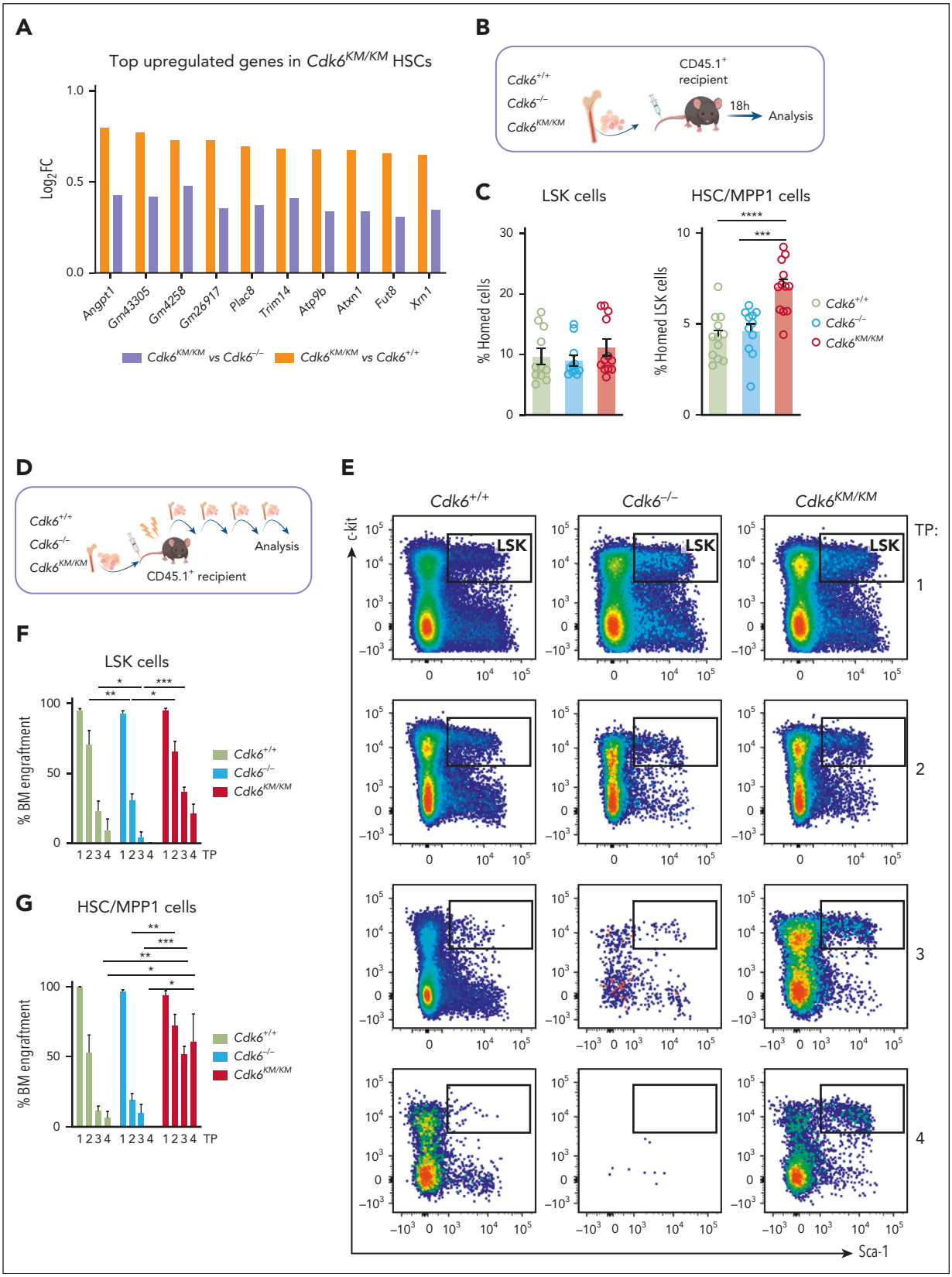

Figure 3. Kinase-inactivated CDK6 enhances HSC homing and self-renewal. (A) Top upregulated genes in dormant *Cdk6*$^{KM/KM}$ HSCs compared with *Cdk6*$^{+/+}$ and *Cdk6*$^{-/-}$ cells from scRNA-seq. (B) Schematic representation of BM homing assay in vivo. (C) Flow cytometry analysis of homed CD45.2^{+} *Cdk6*$^{+/+}$, *Cdk6*$^{-/-}$, and *Cdk6*$^{KM/KM}$ LSK and HSC/MPP1 of LSK cells 18 hours after injection into CD45.1^{+} recipients (n ≥ 11 recipients and donors, mean ± SEM). (D) Serial BM transplantation workflow of *Cdk6*$^{+/+}$, *Cdk6*$^{-/-}$, and *Cdk6*$^{KM/KM}$ BM cells. (E) Representative flow cytometry plots of gated LSK cells over 4 rounds of transplantation (TP). (F-G) Percentage of engrafted CD45.2^{+} *Cdk6*$^{+/+}$, *Cdk6*$^{-/-}$, and *Cdk6*$^{KM/KM}$ LSK and HSC/MPP1 cells over 4 rounds of transplantation. (H) Lineage distribution of engrafted CD45.2^{+} *Cdk6*$^{+/+}$, *Cdk6*$^{-/-}$, and *Cdk6*$^{KM/KM}$ BM cells

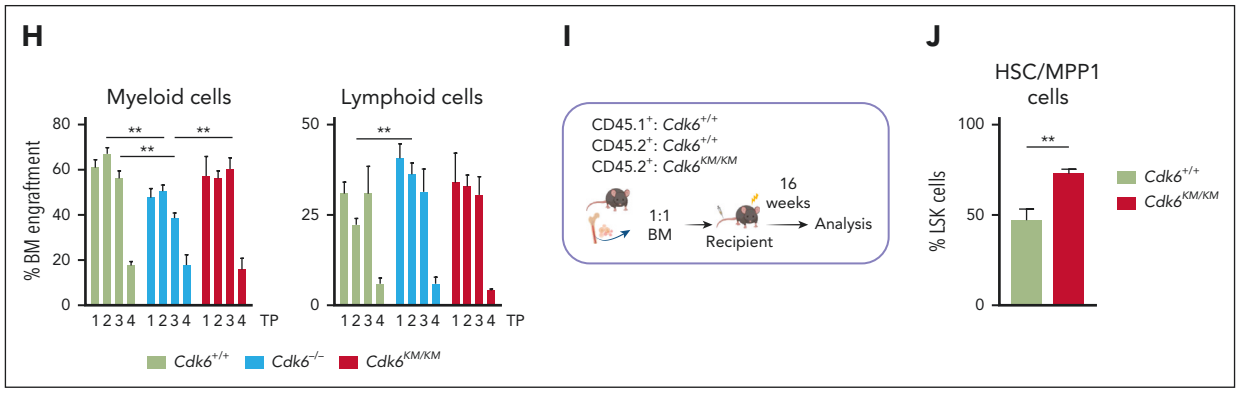

Figure 3 (continued) (n = 3-6/genotype, mean ± SEM). (I) Experimental-design competitive BM transplantation assay, depicting a 1:1 ratio transplantation of CD45.1$^+$ *Cdk6*$^{+/+}$ together with either CD45.2$^+$ *Cdk6*$^{+/+}$ or *Cdk6*$^{KM/KM}$ BM into lethally irradiated recipient mice. (J) End point analysis of competitive transplantation showing CD45.2$^+$ *Cdk6*$^{+/+}$ and *Cdk6*$^{KM/KM}$ HSC/MPP1 cells (n = 7 per group, mean ± SEM). *P < .05; **P < .01; ***P < .001; ****P < .0001.

transcriptional pattern of the dormant *Cdk6*$^{KM/KM}$ HSC subcluster (Figure 1E-G).

The CDK6 protein lacks a DNA-binding domain and acts as a transcriptional cofactor.[7-9,11,14] To understand how CDK6 regulates HSC self-renewal and maintenance, we performed a transcription factor motif analysis in promoter regions of the differentially expressed activation signature genes between kinase-inactivated CDK6 and wild-type CDK6.

NFY and E2F motifs emerged as the most significant findings (Figure 4E). When performing a motif enrichment analysis for the comparison of *Cdk6*$^{-/-}$ with *Cdk6*$^{+/+}$cells, we identified a pattern similar to that of the *Cdk6*$^{KM/KM}$ mutant compared with *Cdk6*$^{+/+}$ cells (Figure 4F). These results validated the canonical cell cycle function of CDK6. Our results also confirmed published data on NFY-A, showing that it is a critical factor in proliferating HSCs.

We recently described that CDK6 phosphorylates NFY-A at serine position S325 in breakpoint cluster region and Abelson chimeric gene (BCR/ABL) transformed cells. Thereby, NFY-A is activated for its transcriptional function.[10]

To validate a CDK6–NFY-A interaction in hematopoietic progenitor cells, we took advantage of our recently established HPC^{LSK} system and generated stem/progenitor cell lines from *Cdk6*$^{+/+}$, *Cdk6*$^{-/-}$, and *Cdk6*$^{KM/KM}$ mice.[23] Subcellular fractionation analysis revealed that kinase-inactivated and wild-type CDK6 protein was comparable in the chromatin and cytoplasmic fractions (Figure 4G) in HPC^{LSK} cells, predicting that kinase-inactivated CDK6 interacts with the chromatin in a similar manner as wild-type CDK6. Coimmunoprecipitation confirmed the protein-protein interaction of CDK6 and NFY-A in *Cdk6*$^{+/+}$ and *Cdk6*$^{KM/KM}$ HPC^{LSK} cells (Figure 4H). To better understand the significance of this interaction, we performed NFY-A short hairpin RNA knockdown experiments with *Cdk6*$^{+/+}$, *Cdk6*$^{-/-}$, and *Cdk6*$^{KM/KM}$ HPC^{LSK} cells. Upon NFY-A knockdown, *Cdk6*$^{KM/KM}$ HPC^{LSK} cells responded with increased cell death compared with *Cdk6*$^{+/+}$ and *Cdk6*$^{-/-}$ cells (supplemental Figure 4B-C). These data are consistent with previous reports that NFY-A loss induces apoptosis and CDK6 kinase activity is needed to antagonize p53-responses.[10,24,25]

Kinase-inactivated CDK6 and MAZ influence HSC maintenance

To identify kinase-inactivated CDK6 interactors maintaining quiescence, we combined motif enrichment analysis with a CDK6 immunoprecipitation–mass spectrometry experiment. We performed motif enrichment analysis of *Cdk6*$^{KM/KM}$ and *Cdk6*$^{-/-}$ deregulated genes compared with *Cdk6*$^{+/+}$ within the quiescent stem cell gene set, and defined *Cdk6*$^{KM/KM}$-specific motifs (Figure 5A-B; supplemental Figure 5A). We performed a nuclear CDK6 immunoprecipitation followed by mass spectrometry analysis with the hematopoietic progenitor cell line HPC-7[26] (Figure 5C). An overlap of these data with the *Cdk6*$^{KM/KM}$-specific motifs highlighted ZNF148, RUNX1, and MAZ as the strongest interactors. The MAZ-CDK6 interaction was validated by proximity ligation assays in *Cdk6*$^{+/+}$ and *Cdk6*$^{KM/KM}$ HSC/MPP1 cells (Figure 5D).

To assess whether CDK6 and MAZ interplay at chromatin, we reanalyzed publicly available chromatin immunoprecipitation sequencing (ChIP-seq) data sets from transformed B cells.[10,27] A total of 9501 binding sites were identified as common peaks for CDK6 and MAZ (Figure 5E-F). The associated CDK6-MAZ bound genes enriched for pathways related to chromatin modification, transcriptional regulation, and apoptotic signaling (supplemental Figure 5B).

The overlap of CDK6-MAZ binding sites with *Cdk6*$^{KM/KM}$ genes upregulated in the HSC subcluster of Figure 1E identified that ~50% of all genes display a common binding site (Figure 5G). Among these 282 genes, several are known HSC mediators (Figure 5H).[17,18,22,28]

Palbociclib (CDK4/6 kinase inhibitor) treatment did not affect MAZ interaction with the promoters of *Mlec*, *Fosb*, and *Hmgb2* in *Cdk6*$^{+/+}$ HPC^{LSK} cells (supplemental Figure 5C). However, CDK6 kinase activity influences the transcription of *Mlec* and *Fosb*, which is abrogated by MAZ knockdown (siMAZ) (supplemental Figure 5D).

MAZ knockdown was performed in sorted LSK cells from *Cdk6*$^{+/+}$ and *Cdk6*$^{KM/KM}$ mice (Figure 5I; supplemental Figure 5E). *Cdk6*$^{KM/KM}$ cells responded with a decrease in HSC/MPP1 cells

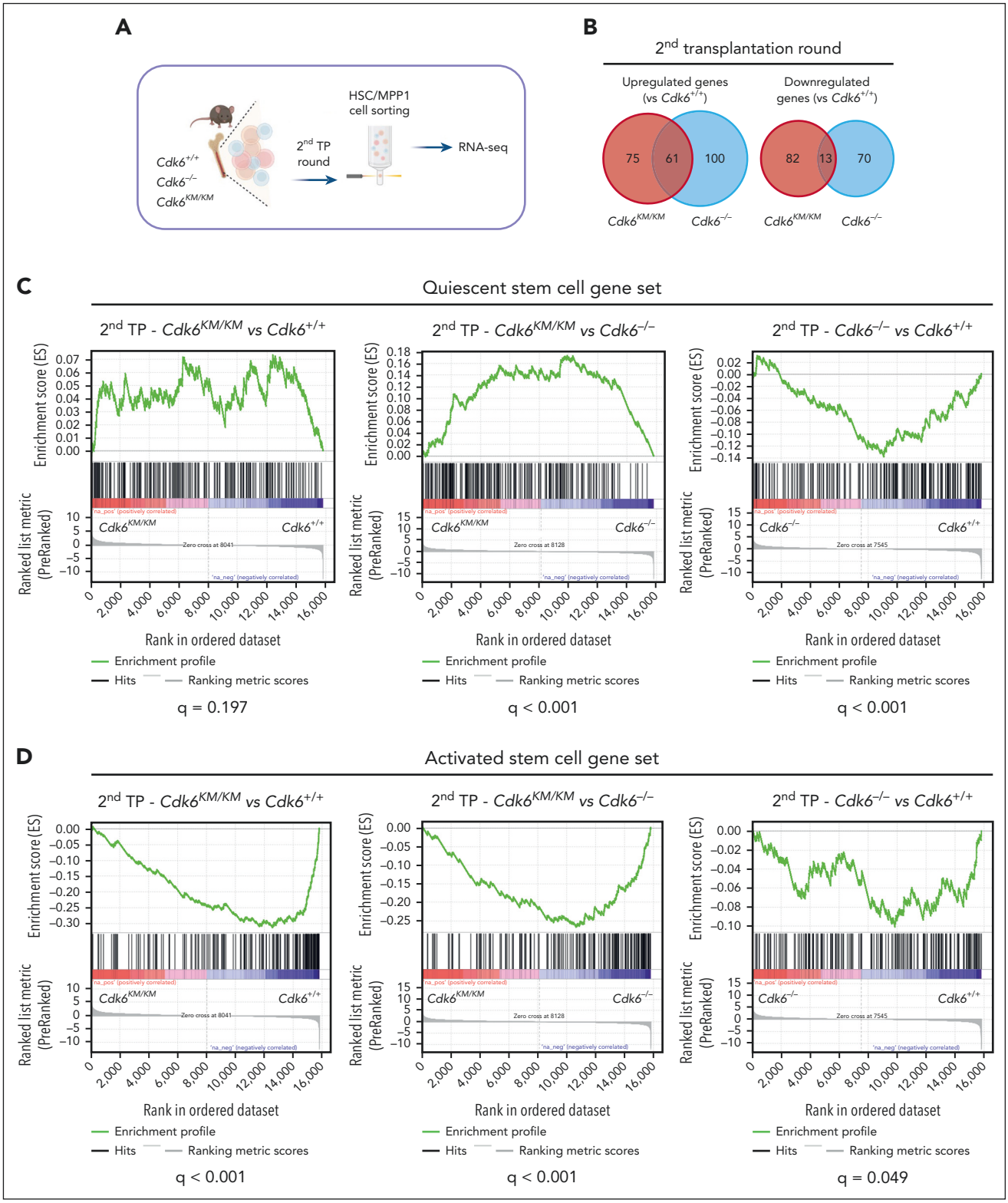

Figure 4. Kinase-inactivated CDK6 balances quiescent and activated transcriptional programs of HSCs. (A) Experimental workflow of low-input RNA-seq of engrafted CD45.2$^+$ HSC/MPP1 cells after 2 serial rounds of transplantation. (B) Venn diagrams showing genes uniquely or commonly upregulated (left) and downregulated (right) in *Cdk6*$^{-/-}$ and *Cdk6*$^{KM/KM}$ compared with *Cdk6*$^{+/+}$ HSC/MPP1 cells after 2 serial rounds of transplantation (n=3; $|\text{Log}_2\text{FC}| \geq 0.3$; adjusted *P* value < .2). (C-D) Gene set enrichment analysis to test for the enrichment of quiescent or activated stem cell gene sets in differentially expressed genes coming from 3 analyses: HSC/MPP1 cells of *Cdk6*$^{KM/KM}$ compared with *Cdk6*$^{+/+}$ cells, *Cdk6*$^{KM/KM}$ compared with *Cdk6*$^{-/-}$, or *Cdk6*$^{-/-}$ compared with *Cdk6*$^{+/+}$ after 2 serial rounds of transplantation. (E-F) Transcription factor motif enrichment analysis of genes within the activated stem cell gene set that are either upregulated in (E) *Cdk6*$^{KM/KM}$ compared with *Cdk6*$^{+/+}$ HSC/MPP1 cells or (F) *Cdk6*$^{-/-}$ compared with *Cdk6*$^{+/+}$ HSC/MPP1 cells upon 2 serial rounds of transplantation. (G) Subcellular fractionation of *Cdk6*$^{+/+}$, *Cdk6*$^{-/-}$, and *Cdk6*$^{KM/KM}$ HPC^{LSK} cells, followed by western blot analysis of CDK6. Lamin B1/regulator of chromosome condensation 1 (RCC1) served as a nuclear marker, whereas heat shock protein 90 (HSP-90) served as a cytoplasmic marker. (H) Anti-NFY-A co-immunoprecipitation (co-IP) from *Cdk6*$^{+/+}$, *Cdk6*$^{-/-}$, and *Cdk6*$^{KM/KM}$ HPC^{LSK} cell extracts followed by NFY-A and CDK6 immunoblotting. IN indicates the input lysate and SN indicates the supernatant after IP. Glyceraldehyde-3-phosphate dehydrogenase (GAPDH) served as loading control.

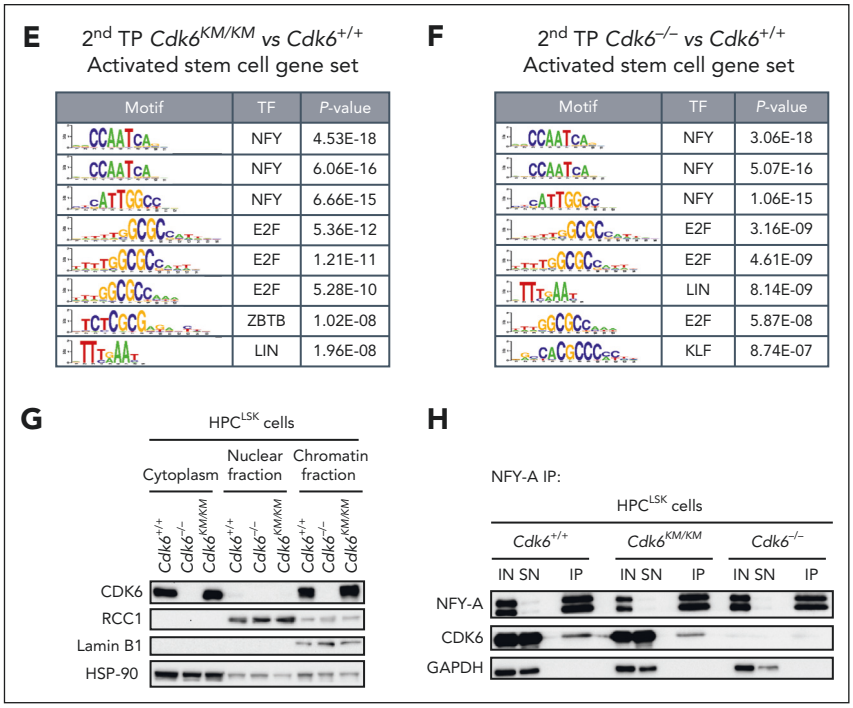

Figure 4 (continued)

compared with controls (Figure 5J-K). Palbociclib-treated *Cdk6*$^{+/+}$ LSK cells with siMAZ yielded comparable results and reduced HSC/MPP1 numbers. The LSK fraction remained unaltered in the different conditions (supplemental Figure 5F). In summary, these data indicate a critical role of the kinase-inactivated CDK6-MAZ axes for HSC maintenance.

CDK4/6 kinase inhibition protects HSC fitness

We used palbociclib to evaluate its effects on *Cdk6*$^{+/+}$ LSK cells by using 10x Genomics scRNA-Seq (Figure 6A).

The integrated data identified 13 individual clusters, which we annotated according to published marker gene expression (Figure 6B; supplemental Figure 6A).[17,18] We further substructured the HSPC cluster and annotated 4 either immature (naïve) or differentiation-prone cell states (Figure 6C; supplemental Figure 6B).[17,18] Consistent with the *Cdk6*$^{KM/KM}$ HSC subcluster (Figure 1D), the palbociclib-treated sample showed a relative increase in cell number of the naïve subcluster compared with control (Figure 6D). To study the above-defined HSC mediators regulated by CDK6 and MAZ (Figure 5G-H), we analyzed the expression of these genes in the naïve subcluster (Figure 6E; supplemental Figure 6C). Top genes identified in Figure 5H, including *Runx1*, *Cd53*, *Stat3*, *Mlec*, and *Cdkn1b*, were found among the top upregulated genes in the naïve palbociclib-treated subcluster relative to controls.

To compare palbociclib-treated LSK cells with CDK6 kinase-inactive cells, we performed an in vivo homing assay. CD45.2^{+} *Cdk6*$^{+/+}$ LSK cells pretreated with palbociclib or the control treatment were injected IV into CD45.1^{+} recipient mice (supplemental Figure 6D-E). At 18 hours after injection, significantly more HSC/MPP1 cells homed in the BM of mice pretreated with palbociclib, whereas LSK cells remained unchanged. MPP2 cells were increased upon palbociclib treatment, whereas MPP3-4 cells were unaltered.

To validate the effects of CDK6 kinase inhibition on the colony-forming potential of HSPCs, we performed serial plating assays with palbociclib (supplemental Figure 6F). Palbociclib treatment resulted in increased colony and LSK cell numbers and decreased differentiated cells from the second round of plating onward.

In vivo treatment with palbociclib every 24 hours over 10 days resulted in a higher percentage of HSC/MPP1-MPP2 cells and reduced MPP 3/4 cells in the BM (Figure 6F-G; supplemental Figure 6G-H). Reduced Myel cells in the BM confirmed the effectiveness of the treatment (supplemental Figure 6I)[29]. HSC/MPP1 cells were embedded for a serial plating assay. Upon the second round of plating, colony and LSK cell numbers of palbociclib-treated mice were enhanced (Figure 6H; supplemental Figure 6J-K).

In combination with a MAZ knockdown, the colony numbers were reduced in the palbociclib and control conditions, whereas the LSK cells were reduced in the palbociclib samples (supplemental Figure 6L-M).

Further, we treated freshly isolated LSK cells either with palbociclib (CD45.2) or PBS (CD45.1) for 72 hours and injected them in a 1:1 ratio into lethally irradiated recipient mice (Figure 6I). After 16 weeks, palbociclib-treated HSC/MPP1 cells showed a competitive advantage (Figure 6J-K; supplemental Figure 6N-O).

To test the effect of palbociclib in a human setting, CD34^{+} cord blood cells were plated with either palbociclib or control in

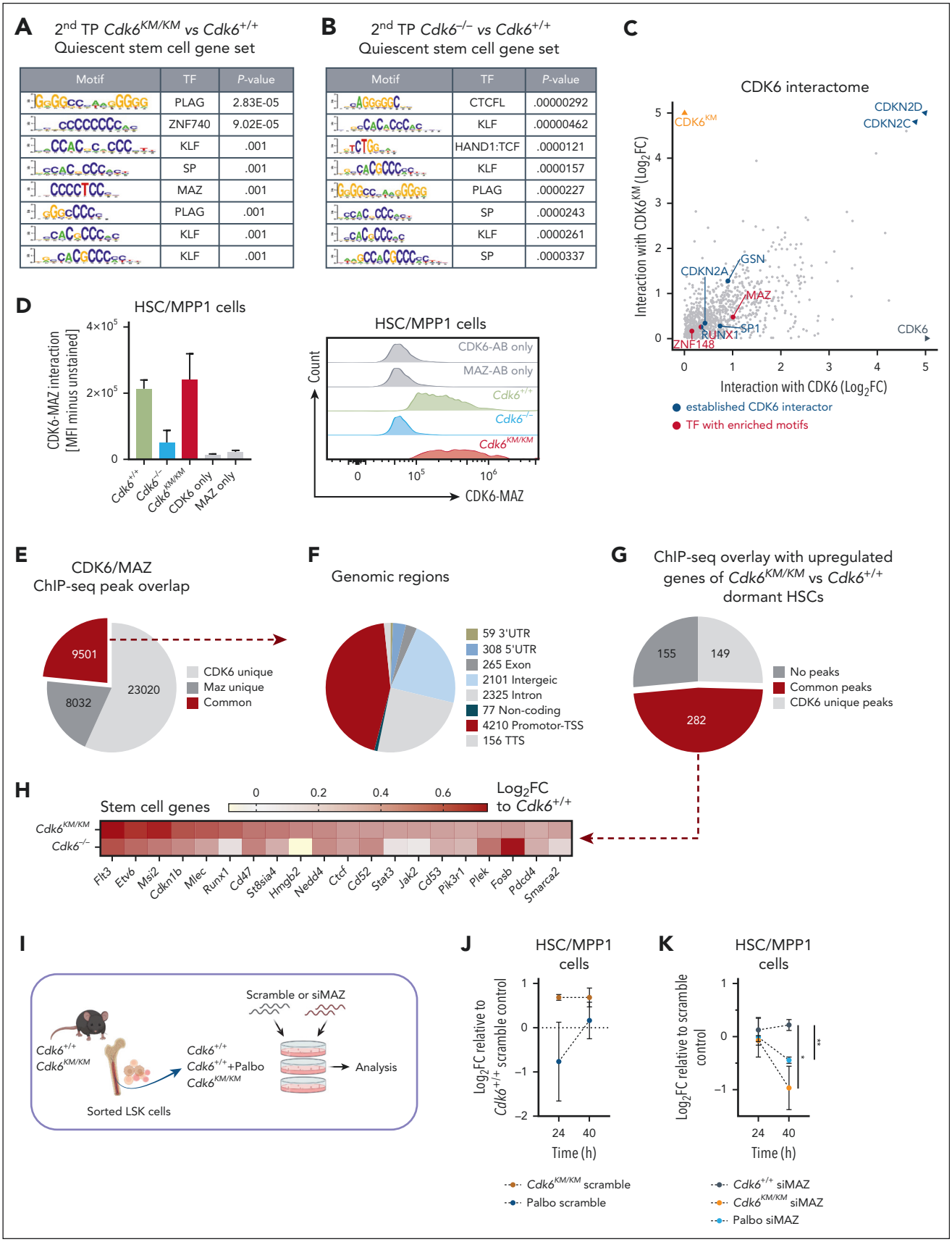

Figure 5. Kinase-inactivated CDK6 and MAZ influence HSC maintenance. (A-B) Transcription factor motif enrichment analysis of genes within the quiescent stem cell gene set that are either upregulated in (A) *Cdk6*$^{KM/KM}$ compared with *Cdk6*$^{+/+}$ cells or (B) *Cdk6*$^{-/-}$ compared with *Cdk6*$^{+/+}$ cells after 2 serial rounds of transplantation. (C) CDK6 interactome analysis generated by nuclear CDK6-IP mass spectrometry analysis of HPC-7 cell lines expressing either wild-type CDK6 or CDK6^{KM}. Dot plot illustrating all

methylcellulose for serial plating assays (Figure 6L). $CD34^+CD38^-$ cells were enriched with palbociclib (Figure 6M-N). The percentage of $CD11b^+$ cells was unaltered (supplemental Figure 6P).

Taken together, our findings demonstrate that sustaining kinase-independent functions of CDK6 in HSCs enables enhanced long-term capacity, which is reflected in a specific transcriptional pattern. Kinase-inactivated CDK6 regulates quiescent and activated stem cell gene sets at least partially with NFY-A and MAZ.

Discussion

The function of the hematopoietic system critically depends on the supply of new cells, which are generated as needed by activation of the HSCs. Many patients suffer from hematopoietic deficiencies, but we lack knowledge of when and how to intervene. HSCT is a potentially curative therapy for various hematopoietic diseases. To enhance the success rate of HSCT, we need to maintain stem cell potential and/or improve homing efficiency.

Homing is one of the multiple processes involved in engraftment, which seems to be partially influenced by CDK6.[30] We propose that CDK4/6 kinase inhibitors could be used to maintain cultured HSCs in their noncycling and naïve state before they are transferred to the recipient. Although the canonical functions of both CDK4 and CDK6 are inhibited, the kinase-independent functions of CDK6 are generally unaffected or even improved. CDK4/6 inhibitors cause a transient arrest of the cell cycle in HSCs, thereby shielding them from chemotherapy-induced damage.[31] We suggest that CDK4/6 inhibitors could be used to treat donor-derived HSCs before HSCT to inhibit their proliferation while improving their regeneration and homing potential.

Critical functions of CDK6 have been described in human cord blood cells. CDK6-enforced expression in long-term HSCs leads to increased cell division, and those cells acquire a competitive advantage that is suggested to be independent of cyclin expression.[32] Loss of CDK6 in HSCs inhibits the cells' exit from dormancy upon activation.[13] We now demonstrate that kinase-inactivated CDK6 influences the transcription of a set of genes to enhance HSC functionality upon long-term activation. These kinase-independent functions of CDK6 might partially explain the effects of long-term HSCs with enforced CDK6 expression, when cyclins are not yet expressed.[32,33] Loss of CDK6 in HSCs shows the opposite effect.

Hu et al found a 50% reduction in LSK cells of $Cdk6^{-/-}$ and $Cdk6^{KM/KM}$ mice compared with $Cdk6^{+/+}$ mice,[14] whereas our analysis failed to detect these differences. This could be caused by stem cells antigen-1 (Sca-1) expression changes. Sca-1 has previously been recognized to react to certain biological stresses,[19] including mouse rearing facilities, with different environmental background in a similar way to the mouse genetic background.

CDK6 does not contain a DNA-binding domain, but exerts its effects by interacting with transcription factors. We have identified the transcription factors with which CDK6 interacts to determine HSC self-renewal. Consistent with our data on leukemic cells,[10] CDK6 interacts with NFY-A in a kinase-dependent manner. The CDK6-NFY-A complex induces a gene set that characterizes activated HSCs. CDK6 and CDK2 phosphorylate the DNA-binding domain of NFY-A.[10,33,34] We have shown that CDK6 interacts with NFY-A in $Cdk6^{+/+}$ and $Cdk6^{KM/KM}$ HSPCs. We postulate that kinase-inactivated CDK6 inhibits NFY-A by interacting with it and preventing its phosphorylation, thereby blocking the transcription of NFY-A–dependent genes and suppressing the progression of HSCs to activated MPP1 cells. Knocking down NFY-A in HSCs with kinase-inactivated CDK6 leads to an increase in apoptosis, which was not observed in HSCs with wild type or lacking CDK6. This might be explained by the fact that both proteins regulate p53-response,[10,24,25] and it underlines the importance of the delicate axis of CDK6 and NFY-A in activated progenitor cells.

The transcription pattern of $Cdk6^{KM/KM}$ HSCs upon transplantation directs the cells to a more quiescent state. The HSC maintenance axis is characterized by a regulating complex including CDK6 and MAZ. The critical role of kinase-inactivated CDK6 and MAZ interaction is supported by MAZ knockdown experiments in HSCs, as HSCs lose their self-renewal ability.

ChIP-Seq data of CDK6 and MAZ from leukemic B cells reveal a large set of common target genes, showing that the role of CDK6 and MAZ is not restricted to healthy hematopoietic cells. We speculate that the effect on MAZ might be due to a scaffolding function or to the blockage of certain phosphorylation sites that are critical for transcriptional inactivation or chromatin release. Similar to CCCTC-Binding Factor (CTCF), MAZ interacts with a subset of cohesins to organize the chromatin.[35]

The transcription factor MAZ provides another possibility to balance differentiation. MAZ binds the promoters of genes related to erythroid differentiation. It is highly expressed in several cancers and regulates angiogenesis via vascular endothelial growth factor (VEGF), another known CDK6 target.[7,9,36-39] MAZ is also a cofactor of CTCF in embryonic stem cells, where it insulates active chromatin at *Hox* clusters during differentiation.[37] This function could explain the bias toward Myel-directed differentiation in $Cdk6^{KM/KM}$ HSPCs, which suggests that CDK6 regulates *Hox* genes and thereby differentiation together with MAZ and CTCF. We thus have evidence for a role

Figure 5 (continued) protein interactions with CDK6 or $CDK6^{KM}$ vs $CDK6^{-/-}$ (Log_2FC). Established CDK6 interactors are highlighted in blue. Transcription factors interacting with $CDK6^{KM}$ and analyzed from the $CDK6^{KM}$ specific motif analysis from supplemental Figure 5A are highlighted in red. (D) Flow cytometry proximity ligation assay of CDK6 and MAZ antibodies showing endogenous protein interaction in ex vivo $Cdk6^{+/+}$, $Cdk6^{-/-}$, and $Cdk6^{KM/KM}$ HSC/MPP1 cells. Representative flow cytometry histograms are depicted on the right. $Cdk6^{-/-}$ cells, MAZ, and CDK6 antibody only samples served as controls. (E) Overlap of CDK6 ChIP-seq data from BCR/ABL^{p185+} cells with published MAZ ChIP-seq data from CH12.LX mouse lymphoma cell line. (F) Annotation of the genomic regions identified in the CDK6/MAZ ChIP-seq overlap. (G) CDK6/MAZ ChIP-seq overlay (+2 kb to –500 bp to transcription start site [TSS]) with upregulated genes of $Cdk6^{KM/KM}$ compared with $Cdk6^{+/+}$ dormant HSC subcluster genes (scRNA-seq FC ≥ 0.3). (H) Stem cell genes of $Cdk6^{KM/KM}$ or $Cdk6^{-/-}$ cells compared with $Cdk6^{+/+}$ cells with a CDK6-MAZ ChIP peak. (I) Experimental design of siRNA MAZ knockdown assay in sorted $Cdk6^{+/+}$LSK cells ± palbociclib treatment and in $Cdk6^{KM/KM}$ LSK cells. (J-K) Flow cytometry analysis of (J) HSC/MPP1 scramble cells and (K) HSC/MPP1 cell subset of LSK cells upon MAZ knockdown ± palbociclib treatment depicted as Log_2FC relative to corresponding scramble controls (n = 4 per genotype, mean ± SEM). *P < .05; **P< .01.

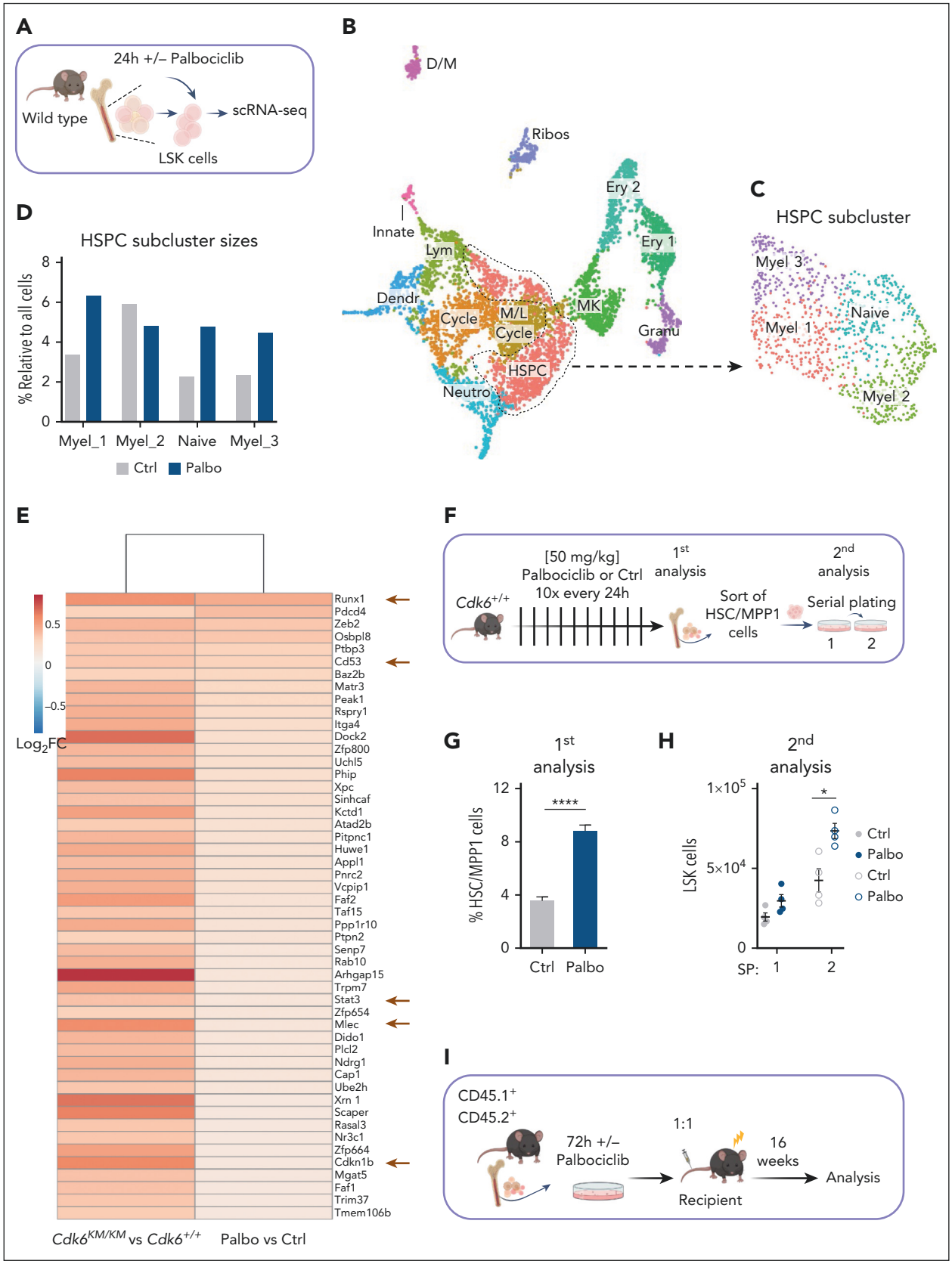

Figure 6. CDK4/6 kinase inhibition protects HSC fitness. (A) Experimental scheme of 10x Genomics scRNA-seq including flow cytometry sorting of LSK cells followed by 24-hour cultivation with either PBS or palbociclib. (B) UMAP visualization of 13 LSK cell clusters. Colors indicate different clusters. (C) UMAP of 4 HSPC subclusters. Myel 1: granulocyte; Myel 2: dendritic; Myel 3: neutrophil; and Naïve: immature cells. (D) Bar chart of relative HSPC subcluster sizes of the PBS or palbociclib-treated samples. (E) Heat map of top 50 upregulated genes upon palbociclib treatment compared with controls out of the 282 genes found in Figure 5G. Errors indicate top genes of Figure 5H, also

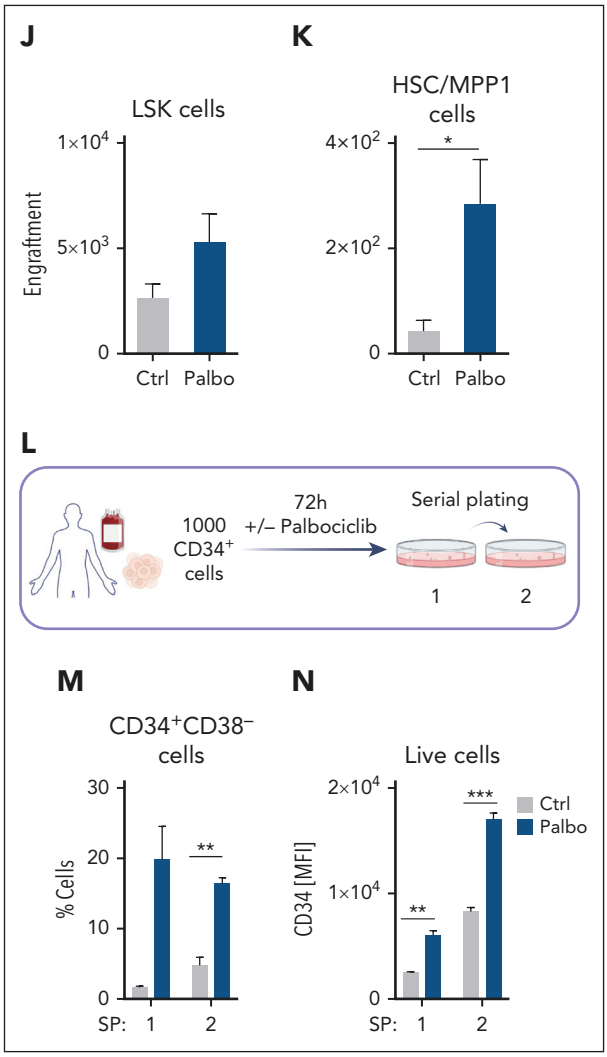

Figure 6 (continued) found in the palbociclib comparison. (F) Experimental design to assess in vivo palbociclib treatment followed by an in vitro serial plating assay of sorted HSC/MPP1 cells. (G) Flow cytometry analysis of HSC/MPP1 cells and (H) serially plated LSK cell numbers upon in vivo palbociclib treatment (n ≥ 4, mean ± SEM). (I) Experimental design for competitive BM transplantation assay. CD45.1$^+$ control and palbociclib-treated (200 nM) CD45.2$^+$ BM cells were transplanted in a 1:1 ratio into lethally irradiated recipient mice upon 72 hours of cultivation. (J-K) End point analysis of engrafted BM LSK and HSC/MPP1 cells upon palbociclib treatment (n = 7 per group, mean ± SEM). (L) Experimental overview of PBS or palbociclib-treated human CD34$^+$ cells followed by a serial plating assay. (M-N) Percentage of CD34$^+$CD38$^-$ cells and mean fluorescence intensity (MFI) of CD34$^+$ cells in 2 serial plating rounds (n = 3-4 per treatment, mean ± SEM). Cycle, cell cycle; Dendr, dendritic; D/M, dendritic/macrophage; Ery, erythroid; Granu, granulocyte; Innate, innate lymphocyte; MK, megakaryocyte; M/L cycle, myeloid/lymphoid cell cycle; Neutro, neutrophil; Ribos, ribosomes; Ctrl, control. *P < .05; **P < .01: ***P< .001; ****P < .0001.

of CDK6 in regulation, not only in the most naïve HSC compartment but also in early hematopoietic progenitors.

Our data indicate a regulation of NFY-A and MAZ by CDK6, which is important for the long-term repopulation capability of HSCs. Our results present a strategy to enhance the success of HSCTs by pretreating HSCs with CDK4/6 kinase inhibitors. CDK4/6 kinase inhibitors are used and tested for combinatorial cancer therapy.[7,40] These treatments might improve the fitness of healthy HSCs as a byproduct of cancer therapy. We highlight CDK6 as a major player in HSPCs, and inactivation of the CDK6 kinase domain thus has dramatically different consequences compared with the complete loss of CDK6. Regarding the upcoming protein degrader strategies, it is crucial for future clinical trials to consider our data showing reduced HSC potential in HSCs lacking CDK6.

Acknowledgments

The authors thank M. Ensfelder-Koperek, P. Kudweis, S. Fajmann, P. Jodl, D. Werdenich, and I. Dhrami for excellent technical support; G. Tebb for his excellent knowledge and support in scientific writing; M. Milsom and F. Grebien for scientific discussions; U. Ma for great technical support and the FACS facility MedUni Vienna for experimental support; and the Biomedical Sequencing Facility at CeMM for next-generation sequencing library preparation, sequencing, and related bioinformatics analyses. This research was supported using resources of the VetCore Facility (Mass Spectrometry) of the University of Veterinary Medicine, Vienna. Graphics were created with BioRender.com

This work was supported by the European Research Council under the European Union's Horizon 2020 research and innovation program (grant agreement No 694354). This research was funded in whole or in part by the Austrian Science Fund (FWF) (SFB-F6101, P 31773).

Authorship

Contribution: I.M.M., E.D., T.K., V.S., and K.K. conceptualized the study; T.K., M.Z., R.G., and G.H. conducted formal analyses; I.M.M., E.D., S.K., L.G., M.P.-M., A.S., L.S., and M.F. performed experiments; U.M., L.E.S., and N.K provided technical support; M.M., A.F., and E.Z.-B. provided resources; I.M.M., E.D., T.K., and K.K. were responsible for writing of the manuscript; and V.S. and K.K. provided supervision.

Conflict-of-interest disclosure: The authors declare no competing financial interests.

ORCID profiles: I.M.M., 0000-0002-9164-9547; E.D., 0000-0003-2989-1022; T.K., 0000-0002-6666-9773; S.K., 0000-0001-7911-9896; A.S., 0000-0001-5446-9136; L.E.S., 0000-0003-2273-7655; A.F., 0000-0002-4628-9052; M.F., 0000-0003-0698-2992; K.K., 0000-0002-7937-4245.

Correspondence: Karoline Kollmann, University of Veterinary Medicine Vienna, Veterinärplatz 1, 1210 Vienna, Austria; email: karoline.kollmann@vetmeduni.ac.at.

Footnotes

Submitted 26 July 2023; accepted 19 April 2024; prepublished online on *Blood* First Edition 29 April 2024. https://doi.org/10.1182/blood.2023021985.

All sequencing data are avaliable via ArrayExpress with the following accession numbers: E-MTAB-13145 (low-input RNA-seq), E-MTAB-13149 (LSK scRNA-seq) and E-MTAB-13268 (Palbociclib LSK cell scRNA-seq).

The online version of this article contains a data supplement.

There is a *Blood* Commentary on this article in this issue.

The publication costs of this article were defrayed in part by page charge payment. Therefore, and solely to indicate this fact, this article is hereby marked "advertisement" in accordance with 18 USC section 1734.

REFERENCES

1. Orkin SH, Zon LI. Hematopoiesis: an evolving paradigm for stem cell biology. *Cell*. 2008;132(4):631-644.
2. Wilson A, Laurenti E, Oser G, et al. Hematopoietic stem cells reversibly switch from dormancy to self-renewal during homeostasis and repair. *Cell*. 2008;135(6):1118-1129.
3. Mayer IM, Hoelbl-Kovacic A, Sexl V, Doma E. Isolation, maintenance and expansion of adult hematopoietic stem/progenitor cells and leukemic stem cells. *Cancers (Basel)*. 2022;14(7):1723-1756.
4. Bazinet A, Popradi G. A general practitioner's guide to hematopoietic stem-cell transplantation. *Curr Oncol*. 2019;26(3):187-191.
5. Yanada M. The evolving concept of indications for allogeneic hematopoietic cell transplantation during first complete remission of acute myeloid leukemia. *Bone Marrow Transplant*. 2021;56(6):1257-1265.
6. Laurenti E, Göttgens B. From haematopoietic stem cells to complex differentiation landscapes. *Nature*. 2018;553(7689):418-426.
7. Nebenfuehr S, Kollmann K, Sexl V. The role of CDK6 in cancer. *Int J Cancer*. 2020;147(11):2988-2995.
8. Handschick K, Beuerlein K, Jurida L, et al. Cyclin-dependent kinase 6 is a chromatin-bound cofactor for NF-κB-dependent gene expression. *Mol Cell*. 2014;53(2):193-208.
9. Kollmann K, Heller G, Schneckenleithner C, et al. A kinase-independent function of CDK6 links the cell cycle to tumor angiogenesis. *Cancer Cell*. 2013;24(2):167-181.
10. Bellutti F, Tigan A-S, Nebenfuehr S, et al. CDK6 antagonizes p53-induced responses during tumorigenesis. *Cancer Discov*. 2018;8(7):884-897.
11. Uras IZ, Maurer B, Nivarthi H, et al. CDK6 coordinates JAK2V617F mutant MPN via NF-kB and apoptotic networks. *Blood*. 2019;133(15):1677-1690.
12. Klein K, Witalisz-Siepracka A, Gotthardt D, et al. T cell-intrinsic CDK6 is dispensable for anti-viral and anti-tumor responses in vivo. *Front Immunol*. 2021;12:650977.
13. Scheicher R, Hoelbl-Kovacic A, Bellutti F, et al. CDK6 as a key regulator of hematopoietic and leukemic stem cell activation. *Blood*. 2015;125(1):90-101.
14. Hu MG, Deshpande A, Schlichting N, et al. CDK6 kinase activity is required for thymocyte development. *Blood*. 2011;117(23):6120-6131.
15. Malumbres M, Sotillo R, Santamaría D, et al. Mammalian cells cycle without the D-type cyclin-dependent kinases Cdk4 and Cdk6. *Cell*. 2004;118(4):493-504.
16. Venezia TA, Merchant AA, Ramos CA, et al. Molecular signatures of proliferation and quiescence in hematopoietic stem cells. *PLoS Biol*. 2004;2(10):e301.
17. Giladi A, Paul F, Herzog Y, et al. Single-cell characterization of haematopoietic progenitors and their trajectories in homeostasis and perturbed haematopoiesis. *Nat Cell Biol*. 2018;20(7):836-846.
18. Rodriguez-Fraticelli AE, Weinreb C, Wang S-W, et al. Single-cell lineage tracing unveils a role for TCF15 in haematopoiesis. *Nature*. 2020;583(7817):585-589.
19. Kanayama M, Izumi Y, Yamauchi Y, et al. CD86-based analysis enables observation of bona fide hematopoietic responses. *Blood*. 2020;136(10):1144-1154.
20. Ito K, Turcotte R, Cui J, et al. Self-renewal of a purified *Tie2* $^{+}$ hematopoietic stem cell population relies on mitochondrial clearance. *Science*. 2016;354(6316):1156-1160.
21. Arai F, Hirao A, Ohmura M, et al. Tie2/angiopoietin-1 signaling regulates hematopoietic stem cell quiescence in the bone marrow niche. *Cell*. 2004;118(2):149-161.
22. Cabezas-Wallscheid N, Klimmeck D, Hansson J, et al. Identification of regulatory networks in HSCs and their immediate progeny via integrated proteome, transcriptome, and DNA methylome analysis. *Cell Stem Cell*. 2014;15(4):507-522.
23. Doma E, Mayer IM, Brandstoetter T, et al. A robust approach for the generation of functional hematopoietic progenitor cell lines to model leukemic transformation. *Blood Adv*. 2021;5(1):39-53.
24. Gatta R, Dolfini D, Mantovani R. NF-Y joins E2Fs, p53 and other stress transcription factors at the apoptosis table. *Cell Death Dis*. 2011;2(5):e162.
25. Bungartz G, Land H, Scadden DT, Emerson SG. NF-Y is necessary for hematopoietic stem cell proliferation and survival. *Blood*. 2012;119(6):1380-1389.
26. Pinto do O P, Kolterud A, Carlsson L. Expression of the LIM-homeobox gene LH2 generates immortalized Steel factor-dependent multipotent hematopoietic precursors. *EMBO J*. 1998;17(19):5744-5756.
27. Yue F, Cheng Y, Breschi A, et al. A comparative encyclopedia of DNA elements in the mouse genome. *Nature*. 2014;515(7527):355-364.
28. Busch K, Klapproth K, Barile M, et al. Fundamental properties of unperturbed haematopoiesis from stem cells in vivo. *Nature*. 2015;518(7540):542-546.
29. Bisi JE, Sorrentino JA, Jordan JL, et al. Preclinical development of G1T38: A novel, potent and selective inhibitor of cyclin dependent kinases 4/6 for use as an oral antineoplastic in patients with CDK4/6 sensitive tumors. *Oncotarget*. 2017;8(26):42343-42358.
30. Lapidot T, Dar A, Kollet O. How do stem cells find their way home? *Blood*. 2005;106(6):1901-1910.
31. He S, Roberts PJ, Sorrentino JA, et al. Transient CDK4/6 inhibition protects hematopoietic stem cells from chemotherapy-induced exhaustion. *Sci Transl Med*. 2017;9(387):eaal3986.

32. Laurenti E, Frelin C, Xie S, et al. CDK6 levels regulate quiescence exit in human hematopoietic stem cells. *Cell Stem Cell*. 2015;16(3):302-313.

33. Farina A, Manni I, Fontemaggi G, et al. Down-regulation of cyclin B1 gene transcription in terminally differentiated skeletal muscle cells is associated with loss of functional CCAAT-binding NF-Y complex. *Oncogene*. 1999 6; 18(18):2818-2827.

34. Yun J, Chae H-D, Choi T-S, et al. Cdk2-dependent phosphorylation of the NF-Y transcription factor and its involvement in the p53-p21 signaling pathway. *J Biol Chem*. 2003;278(38):36966-36972.

35. Xiao T, Li X, Felsenfeld G. The Myc-associated zinc finger protein (MAZ) works together with CTCF to control cohesin positioning and genome organization. *Proc Natl Acad Sci U S A*. 2021;118(7): e2023127118.

36. Deen D, Butter F, Daniels DE, et al. Identification of the transcription factor MAZ as a regulator of erythropoiesis. *Blood Adv*. 2021;5(15):3002-3015.

37. Ortabozkoyun H, Huang P-Y, Cho H, et al. CRISPR and biochemical screens identify MAZ as a cofactor in CTCF-mediated insulation at Hox clusters. *Nat Genet*. 2022; 54(2):202-212.

38. Triner D, Castillo C, Hakim JB, et al. Myc-associated zinc finger protein regulates the proinflammatory response in colitis and colon cancer via STAT3 signaling. *Mol Cell Biol*. 2018;38(22):e00386-18.

39. Yu Z-H, Lun S-M, He R, et al. Dual function of MAZ mediated by FOXF2 in basal-like breast cancer: promotion of proliferation and suppression of progression. *Cancer Lett*. 2017;402:142-152.

40. Fassl A, Geng Y, Sicinski P. CDK4 and CDK6 kinases: from basic science to cancer therapy. *Science*. 2022;375(6577):eabc1495.